

# Prominent effect of soil network heterogeneity on microbial invasion

F.J. Pérez-Reche,<sup>1</sup> S.N. Taraskin,<sup>2</sup> W. Otten,<sup>1</sup> M.P. Viana,<sup>3</sup> L. da F. Costa,<sup>3</sup> and C.A. Gilligan<sup>4</sup>

<sup>1</sup>*SIMBIOS Centre, University of Abertay, Dundee, UK*

<sup>2</sup>*St. Catharine's College and Department of Chemistry, University of Cambridge, Cambridge, UK*

<sup>3</sup>*Instituto de Física de Sao Carlos, Universidade de Sao Paulo, Sao Carlos, SP, Brazil*

<sup>4</sup>*Department of Plant Sciences, University of Cambridge, Cambridge, UK*

Using a network representation for real soil samples and mathematical models for microbial spread, we show that the structural heterogeneity of the soil habitat may have a very significant influence on the size of microbial invasions of the soil pore space. In particular, neglecting the soil structural heterogeneity may lead to a substantial underestimation of microbial invasion. Such effects are explained in terms of a crucial interplay between heterogeneity in microbial spread and heterogeneity in the topology of soil networks. The main influence of network topology on invasion is linked to the existence of long channels in soil networks that may act as bridges for transmission of microorganisms between distant parts of soil.

Understanding how the ubiquitous structural heterogeneity of natural habitats affects the movement and spatial distribution of biota is an important and fascinating question relevant to several disciplines [1, 2]. In particular, the soil pore space is a highly heterogeneous habitat hosting a stunning wealth of biological activity (e.g. of bacteria, fungi or nematodes [3–5]) that plays an essential role in many processes including plant growth [6], climate change [7], or soil-borne epidemics [8]. The study of the interplay between soil structural heterogeneity and microbial activities in three dimensions (3D) is challenging due to the opacity of soil and the complexity of biological and environmental factors involved in microbial spread. Experiments based on soil thin sections [9–13] or planar microcosms [9, 14, 15] give some insight. For instance, it was observed that the volume of soil explored by fungi increases with the soil bulk density [12] and macropores may act as either preferential pathways or barriers for fungal spread [13]. However, due to the nature of the techniques, these type of experiments fail to provide information in 3D so as to quantitatively assess the influence of the structural heterogeneity and topology on microbial invasion. Current understanding based on ecological and epidemiological models suggests that heterogeneity in soil structure could either enhance or reduce the probabilities of invasions [16–19]. The outcome depends largely on the properties of the pore space, including the connectivity and pore sizes, and the effects these properties have on microbial movement through soil. In this letter, we identify the main structural factors that affect invasion by devising several network models for biological invasion with increasing degree of interplay between microbial spread and the structure of the soil pore space (Table I). Our results and conclusions are not only relevant to biological invasion in soil but are also expected to be important for any biota moving in complex landscapes or generic agents spreading in networks with structurally complex links.

We have analysed the invasion models for six real soil samples: three samples of soil without tillage treat-

ment (denoted as N1, N2, and N3) and three samples of ploughed soil (P1, P2, and P3). The main qualitative difference between N and P samples is that the pores are typically larger in the P samples (see Fig. 1(a) and the statistical analysis in [20]). For our theoretical analysis, we have used a network representation of the soil pore structure derived from 3D-digital images of the soil samples scanned with an X-ray micro-tomography device [20]. Soil networks consist of a set of nodes and edges whose layout captures the topology of the soil pore space where biological activity takes place. The network representation is achieved by associating the branching points of the soil pore space with the nodes and the pore-space channels between branching points with the network edges (see [20] for more detail and a comparison with previously proposed network representations for soil [21–24]). Fig. 1(b) shows the network for sample N1. All the networks have similar topological properties irrespective of tillage treatment (Table II). The samples exhibit limited node degree, small topological heterogeneity, high clustering in comparison with random graphs, and *fractal* small-world behaviour (i.e. the mean separation between nodes increases as  $\langle l \rangle \sim N^\eta$  with  $\eta \simeq 0.4$ , which contrasts with the slower increase  $\langle l \rangle \sim \ln N$  in standard small-world networks [25]). Such features are typical for geographical networks embedded in Euclidean spaces [26, 27] and are thus not un-expected for soil networks that are embedded in a 3D space. The connectivity in this kind of networks is limited because each edge fills a certain space and thus the number of edges per node is restricted [20, 26, 27]. This property remains unaltered under tillage and this is likely to be the reason why the topologies are statistically similar for both N and P samples. We describe the structure of channels in terms of their arc-length,  $L$ , and local cross-section area  $S(x)$  (Fig. 1). Both the mean value  $\langle L \rangle$  and the relative dispersion  $\sigma_L^2/\langle L \rangle^2$  of the arc-length are similar for all the samples (Table II). A relatively weak heterogeneity in  $L$ , i.e.  $\sigma_L^2/\langle L \rangle^2 < 1$ , contrasts with much greater variability in the cross-section area along chan-

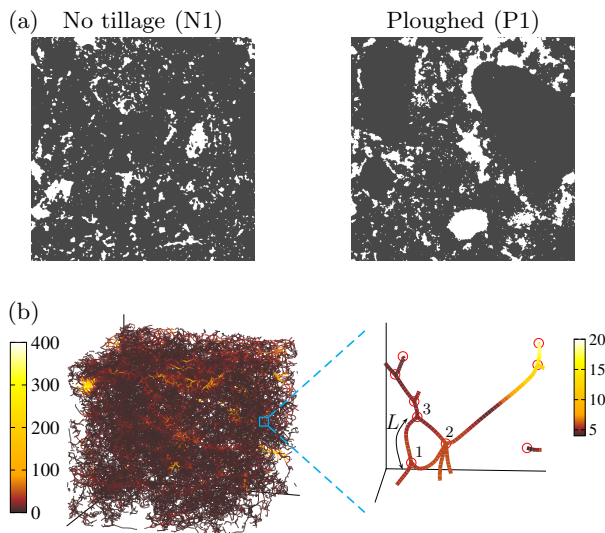


FIG. 1. Soil samples and soil networks. (a) 2D-sections of 3D-digital images of soil samples N1 and P1 (sample size:  $3.5 \times 3.5 \times 3.5$  cm). The pore space and solid matrix are shown in white and grey colours, respectively. (b) Network representing the pore space of sample N1. The colour of channels indicates their local cross-section area,  $S(x)$ , where  $x$  gives the position along channels. The zoom on the right illustrates the definition of the arc-length of channels,  $L$ , the node degree heterogeneity, and clustering (triangle 1-2-3) (cf. Table II). Both  $L$  and  $S(x)$  are dimensionless, i.e. scaled by the size of voxel in the 3D-digital image.

nels, i.e.  $\sigma_S^2/\langle S \rangle^2 > 1$ . Large cross-sections are typical for long channels which are frequently attached to nodes with large  $k$ . Spatial correlations of  $S(x)$  are significant (i.e. narrow channels tend to be attached to narrow channels and vice-versa) [20]. Here, we show that the heterogeneity in  $S(x)$ , the correlations between  $L$  and  $S(x)$  and spatial correlations for  $S(x)$  play a key role for microbial invasion.

The spread of micro-organisms through a given pore space in soil is not a deterministic process but it occurs with certain probability [8, 9]. Inspired by epidemiological network models [17–19, 30–32], we assume that microorganisms reaching a node in the soil network are able to colonise any of the channels that emerge from that node and to reach uncolonised nodes with probability  $T$  (referred to as the transmissibility). This quantity is central for all the models proposed in this work. Each model assumes a different form for  $T$  (Table I). *Model 1* corresponds to the simplest mean-field case with  $T$  being identical for all the channels. In *model 2*,  $T$  is independent of the structural properties of channels but it takes a random value for each channel (representing, e.g. a non-uniform spatial distribution of nutrient resources necessary for microbial activity [33]) that obeys a bi-modal distribution parameterised by the mean transmissibility,  $\langle T \rangle$ . *Model 3* suggests that  $T$  depends on the arc-length

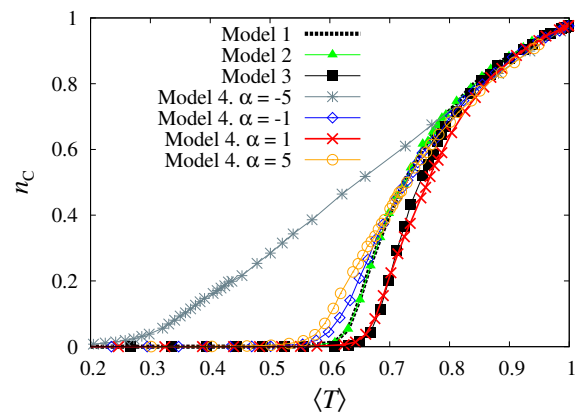


FIG. 2. Invasion in soil networks. The vertical axis displays the density of colonisation,  $n_C$ , in network N1 averaged over  $10^4$  invasions starting from different randomly chosen nodes. The horizontal axis shows the mean transmissibility of microbes,  $\langle T \rangle$ , obtained by averaging over channels. Different curves correspond to invasions predicted by different models (and exploration controlled by  $\alpha$  in model 4).

of channels ( $L$ ) and the spatial scale of microbial colonisation is characterised by a typical exploration length,  $\lambda_0$ . The value of transmissibility is assumed to decay with increasing  $L$ , meaning that microbial transmission through short channels is more likely than through longer channels. In *Model 4*,  $T$  depends on both  $L$  and the cross-section area along channels,  $S(x)$ . The dependence on  $L$  is again controlled by the parameter  $\lambda_0$ . Regarding  $S(x)$ , we keep our description general so as to account both for microorganisms with preferential spread through pores with wide cross-sections and those that have a preference for narrow cross-sections. This preference may depend on a combination of biological and physical factors such as competitive exclusion from pore-size classes due to predator-prey interactions [1, 3, 16], or the spatial distribution of water in soil [3, 9, 10, 15]. We capture these factors qualitatively with an effective area exploration parameter,  $\alpha$ , whose sign controls the preference for narrow ( $\alpha > 0$ ) or wide ( $\alpha < 0$ ) cross-sections. For  $\alpha = 0$ , model 4 reduces to model 3 (cf. expressions for  $T$  in Table I).

We quantify the size of invasion by the density of colonisation,  $n_C$ , defined as the relative number of nodes reached by the microbial colony during an invasion that starts from a randomly chosen node in the network. Numerical simulations reveal that the mean value of  $n_C$  predicted by model 1 increases with  $T$  but only takes significantly large values (e.g.  $n_C \gtrsim 0.1$ ) if  $T > T_c$ , where  $T_c \simeq 0.6$  for all the analysed networks (Fig. 2 and [20]). Similar threshold behaviour for invasion is typically observed in some epidemiological models [17–19, 30–32]. The heterogeneity in  $T$  considered in model 2 does not introduce significant differences to  $n_C$  which coincides with that for model 1 if the strength of microbial transmis-

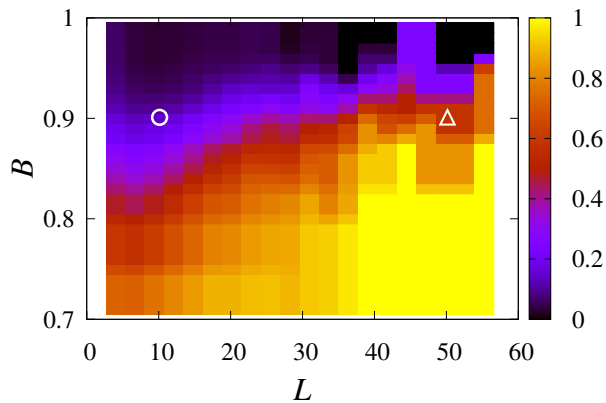


FIG. 3. Bridging effect for edges in network N1. The colour along the vertical direction gives the fraction of edges with given  $L$  (i.e. fixed value on the horizontal axis) whose degree of bridging is larger than the value  $B$  plotted along the vertical axis. For instance, the colour inside the circle (triangle) indicates that the fraction of channels of length  $L = 10$  ( $L = 50$ ) with  $B > 0.9$ , i.e.  $l_b > 10$ , is approximately 0.1 (0.7). By definition,  $B \in [0, 1]$  but only values of  $B > 0.7$  are shown to highlight the variation in  $B$  with  $L$ . Channels attached to border nodes of degree 1 are not included in the graph. See [20] for similar plots for other soil samples.

sion is parametrised by  $\langle T \rangle$  in both models. This result holds in general if the values of  $T$  for all the channels in the network are statistically independent from each other [34, 35]. For given  $\langle T \rangle$ , model 3 predicts colonisations of smaller size on average than that for model 1 (the colonisation curve for model 3 is clearly below the curve for model 1 in Fig. 2). Therefore, heterogeneity in  $T$  induced by heterogeneity in  $L$  makes the soil network more resilient to microbial invasion [36]. Model 4 predicts a similar behaviour for values of  $\alpha$  near zero which is expected since models 4 and 3 coincide for  $\alpha = 0$  (see, e.g. the invasion curve for  $\alpha = 1$  in Fig. 2). In contrast, for larger values of the area exploration parameter (either  $\alpha > 0$  or  $\alpha < 0$ ), invasions for given  $\langle T \rangle$  can be more significant in model 4 than in any of the other models. The effect is especially pronounced for large negative  $\alpha$  (compare, e.g. the curve for  $\alpha = -5$  with that for homogeneous  $T$  in Fig. 2). This is a clear illustration of the prominent effect of the strong heterogeneity in cross-sections of soil channels on biological invasion.

The above results can be understood in terms of the intuitive idea that some channels act as bridges that link nodes that would otherwise be further apart or disconnected. Accordingly, if some microorganisms are able to colonise channels with high “bridging-effects”, the resulting invasions should be large. This behaviour is reminiscent of the small-world effect [29, 34] and is related to the fractal small-world property of soil networks [25]. In order to quantify the bridge effect for every pair,  $u-v$ , of connected nodes we measure the range of the edge  $u-v$

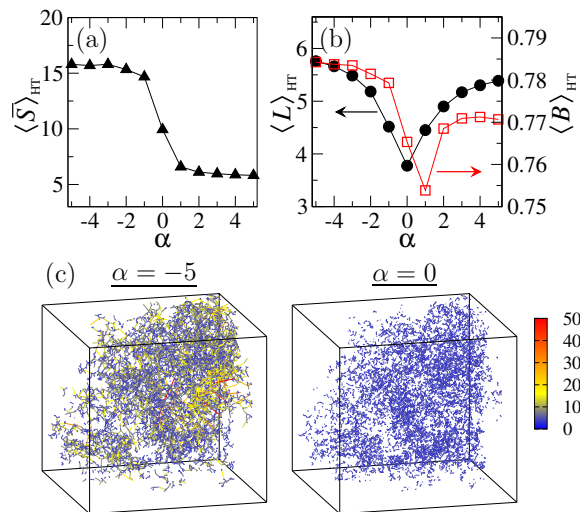


FIG. 4. (a) Mean cross-section area of channels,  $\langle \bar{S} \rangle_{HT}$ , (b) mean arc-length,  $\langle L \rangle_{HT}$  and mean bridgeness,  $\langle B \rangle_{HT}$ , obtained by averaging over channels with high transmissibility (HT,  $T > \langle T \rangle$ ) in sample N1 for microbes with  $\langle T \rangle = 0.5$ . (c) Plots of the channels with  $T > 0.5$  coloured according to their value of  $L$ .

[37] which gives the number of links,  $l_b$ , along the shortest path from  $u$  to  $v$ , if the edge linking these two nodes is removed and define the bridgeness,  $B$ , as  $B = 1 - 1/l_b$ . Channels with  $B$  close to unity indicate the presence of bridges for transmission because the shortest alternative path has a large number of steps,  $l_b$ . Fig. 3 shows that  $B$  is heterogeneous but is correlated with the channel length, typically taking larger values for channels with long arc-length. This effect is ultimately responsible for the variations between invasion curves in Fig. 2 for different models.

In models 1 and 2 for invasion,  $T$  is not linked to the structural properties of channels and is thus independent of  $B$ . In contrast, model 3 assumes that  $T$  decays monotonically with  $L$  meaning that microorganisms are more likely to be transmitted through short channels which typically have small  $B$  (rather than through channels of any length as in models 1 and 2). This explains why the typical size of invasions for given  $\langle T \rangle$  is smaller in model 3 than predicted by models 1 and 2. In contrast, the transmissibility in model 4 depends on  $S(x)$  (provided  $\alpha \neq 0$ ) and does not decay monotonically with  $L$  as in model 3 (see Sec. VI in [20]). As a result, some long channels with high degrees of bridging are able to transmit microbes more efficiently than other with smaller  $L$  and  $B$ . Fig. 4 illustrates this idea for microbial invasion with given  $\langle T \rangle = 0.5$  by showing that the cross-section area of highly transmissible channels with  $T > \langle T \rangle$  decreases with  $\alpha$  (Fig. 4(a)) but their length and bridgeness show a minimum for  $\alpha = 0$  (Fig. 4(b) and (c)). The larger values of  $B$  observed for  $\alpha < 0$  (i.e. when wide channels are

preferred) are due to the positive correlations between  $S(x)$  and  $L$ . In spite of these correlations, invasions with positive  $\alpha$  (preference for narrow channels) may have a large value of  $B$  because  $S(x)$  is very heterogeneous and there are channels that are both narrow and long [20]. The invasions corresponding to  $\alpha \neq 0$  are then typically larger than predicted by models 1-3 (Fig. 2). The effect is particularly important for  $\alpha < 0$  because wide channels (preferred for  $\alpha < 0$ ) tend to be longer than narrow channels. Similarly, the significant spatial correlations in  $S$  favour invasion in model 4 (see [20]).

According to our analysis, the global traits of invasion are mainly dictated by generic characteristics such as the heterogeneity in the network (i.e. in channel length and degree of bridging) and transmission. An important conclusion which applies to invasions in any heterogeneous landscape is that a limited parametrisation of microbial transmission (e.g. in terms of  $\langle T \rangle$ ) combined with an insufficient description of structural heterogeneity in models (e.g. as in models 1-3) may lead to serious underestimates of the size of invasions. This highlights the importance of capturing (i) the essential features of structural heterogeneity that affect microbial spread and (ii) the appropriate parametrisation of microbial transmission which takes into account the effects of structural heterogeneity. Our results suggest that describing microbial transmission in terms of the parameters  $\lambda_0$  and  $\alpha$  (Model 4) is more appropriate than using just  $\langle T \rangle$ . Indeed,  $\lambda_0$  and  $\alpha$  give a better description of the effects of channel structure on microbial spread and reveal significant differences in invasion for ploughed and unploughed soil (microorganisms with preference for wide channels invade more in ploughed soil, and vice versa [20]).

To conclude, our work demonstrates that the shape, size, and interconnection of pores in addition to other characteristics influencing the value of the area exploration parameter  $\alpha$  (e.g. type of microorganisms) are the key factors determining the extend of microbial invasion in soil. The interplay between heterogeneity in microbial transmission and heterogeneity in the topology of soil networks plays a crucial role for biological invasions in soil.

We acknowledge fruitful discussions with V.L. Morales. CAG gratefully acknowledges support for a BBSRC Professorial Fellowship. LdFC is grateful to FAPESP (05/00587-5) and CNPq (301303/06-1 and 573583/2008-0). MPV thanks FAPESP (2010/16310-0) for his post-doc grant.

---

[1] M. Turner, R. Gardner, and R. O'Neill, *Landscape ecology in theory and practice: pattern and process* (Springer, 2001)

[2] G. M. Viswanathan, M. G. E. da Luz, E. P. Raposo, and H. E. Stanley, *The physics of foraging* (Cambridge University Press, Cambridge, UK, 2011)

[3] P. Lavelle and A. Spain, *Soil Ecology* (Springer, 2001)

[4] J. Copley, *Nature* **406**, 452 (2000)

[5] I. M. Young and J. W. Crawford, *Science* **304**, 1634 (2004)

[6] E. T. Kiers, M. Duhamel, Y. Beesetty, J. A. Mensah, O. Franken, E. Verbruggen, C. R. Fellbaum, G. A. Kowalchuk, M. M. Hart, A. Bago, T. M. Palmer, S. A. West, P. Vandenkoornhuys, J. Jansa, and H. Bcking, *Science* **333**, 880 (2011), <http://www.sciencemag.org/content/333/6044/880.full.pdf>

[7] P. S. B. K. Singh, R. D. Bardgett and D. S. Reay, *Nat Rev Micro* **8**, 779 (2010)

[8] W. Otten and C. A. Gilligan, *European Journal of Soil Science* **57**, 26 (2006)

[9] R. B. Franklin and A. L. Mills, eds., *The Spatial Distribution of Microbes in the Environment* (Springer, Dordrecht, 2007)

[10] W. Otten and C. A. Gilligan, *New Phytol.* **138**, 629 (1998)

[11] N. Nunan, K. Wu, I. Young, J. Crawford, and K. Ritz, *Microbial Ecology* **44**, 296 (2002), 10.1007/s00248-002-2021-0

[12] K. Harris, I. M. Young, C. A. Gilligan, W. Otten, and K. Ritz, *FEMS Microbiology Ecology* **44**, 45 (2003)

[13] W. Otten, K. Harris, I. Young, K. Ritz, and C. Gilligan, *Soil Biology and Biochemistry* **36**, 203 (2004)

[14] S. Hapca, J. Crawford, and I. Young, *J. Roy. Soc. Interface* **6**, 111 (2009)

[15] A. Dechesne, G. Wang, G. Glez, D. Or, and B. F. Smets, *Proceedings of the National Academy of Sciences* **107**, 14369 (2010), <http://www.pnas.org/content/107/32/14369.full.pdf+html>

[16] B. A. Melbourne, H. V. Cornell, K. F. Davies, C. J. Dugaw, S. Elmendorf, A. L. Freestone, R. J. Hall, S. Harrison, A. Hastings, M. Holland, M. Holyoak, J. Lambriños, K. Moore, and H. Yokomizo, *Ecology Letters* **10**, 77 (2007)

[17] F. M. Neri, F. J. Pérez-Reche, S. N. Taraskin, and C. A. Gilligan, *J. Roy. Soc. Interface* **8**, 201 (2011)

[18] M. E. J. Newman, *Phys. Rev. E* **66**, 016128 (2002)

[19] J. C. Miller, *Phys. Rev. E* **76**, 010101 (2007)

[20] See supplemental material at <http://link.aps.org/supplemental/xxxx> for further details on methods and results.

[21] H. J. Vogel and K. Roth, *European Journal of Soil Science* **49**, 547 (1998)

[22] H.-J. Vogel and K. Roth, *Advances in Water Resources* **24**, 233 (2001)

[23] A. Santiago, J. P. Cárdenas, J. C. Losada, R. M. Benito, A. M. Tarquis, and F. Borondo, *Nonlinear Processes in Geophysics* **15**, 893 (2008)

[24] J. Cárdenas, A. Santiago, A. Tarquis, J. Losada, F. Borondo, and R. Benito, *Geoderma* **160**, 13 (2010)

[25] G. Csányi and B. Szendrői, *Phys. Rev. E* **70**, 016122 (2004)

[26] S. Boccaletti, V. Latora, Y. Moreno, M. Chavez, and D. Hwang, *Phys. Rep.* **424**, 175 (2006)

[27] J. Buhl, J. Gautrais, R. Solé, P. Kuntz, S. Valverde, J. Deneubourg, and G. Theraulaz, *Eur. Phys. J. B* **42**, 123 (2004)

[28] A. Barrat, M. Barthélemy, and A. Vespignani, *Dynamical Processes on Complex Networks* (Cambridge University Press, Cambridge, 2008)

[29] D. J. Watts and S. H. Strogatz, *Nature* **393**, 440 (1998)

- [30] P. Grassberger, *Math. Biosc.* **63**, 157 (1983)
- [31] F. J. Pérez-Reche, J. J. Ludlam, S. N. Taraskin, and C. A. Gilligan, *Phys. Rev. Lett.* **106**, 218701 (2011)
- [32] A. Vespignani, *Nat Phys* **8**, 32 (2012)
- [33] C. H. Ettema and D. A. Warde, *Trends Ecol. Evol.* **17**, 177 (2002)
- [34] L. Sander, C. P. Warren, I. M. Sokolov, C. Simon, and J. Koopman, *Math. Biosc.* **180**, 293 (2002)
- [35] F. J. Pérez-Reche, S. N. Taraskin, L. d. F. Costa, F. M. Neri, and C. A. Gilligan, *J. Roy. Soc. Interface* **7**, 1083 (2010)
- [36] F. Perez-Reche, S. Taraskin, F. Neri, C. Gilligan, L. da F. Costa, M. Viana, W. Otten, and D. Grinev, in *Proc. 16th International Conference on Digital Signal Processing* (2009) pp. 1–8
- [37] A. E. Motter, T. Nishikawa, and Y.-C. Lai, *Phys. Rev. E* **66**, 065103 (2002)

TABLE I. Models for microbial spread.  $T$  is the transmissibility.  $L$  ( $S$ ) is the arc-length (cross-section) of channels.  $\lambda_0$  ( $\alpha$ ) is the length (area) exploration parameter.  $\overline{S^\alpha} = L^{-1} \int_0^L [S(x)]^\alpha dx$  is the average of  $S(x)^\alpha$  along channels. Derivations of  $T$  for models 3 and 4 are presented in [20].

Model	Heterogeneity	Parameters	Transmissibility
1	None	$T$	$T$
2	Non-structural	$\langle T \rangle$	$\begin{cases} 0, & \text{with Prob } 1 - \langle T \rangle \\ 1, & \text{with Prob } \langle T \rangle \end{cases}$
3	$L$	$\lambda_0$	$\exp(-L/\lambda_0)$
4	$L, S(x)$	$\lambda_0, \alpha$	$\exp(-L \overline{S^\alpha}/\lambda_0)$

TABLE II. Network topological characteristics and channel properties for six soil samples.  $N$  and  $E$  denote the number of nodes and the number of edges in networks, respectively.  $\langle k \rangle$  is the mean degree and  $\sigma_k^2/\langle k \rangle^2 = \langle k^2 \rangle/\langle k \rangle^2 - 1$  is a measure of the topological heterogeneity [28]. The clustering  $C$  is given relative to  $C_{\text{rand}} = \langle k \rangle/N$  for a random graph with the same value of  $N$  and  $\langle k \rangle$  [29]. The mean separation length,  $\langle l \rangle$ , gives the typical separation between two nodes in the network [29].  $\langle L \rangle$  and  $\sigma_L^2/\langle L \rangle^2$  are the mean value and dispersion of  $L$ . Analogous quantities for cross-section area  $S$  are given in the last two columns.

Sample	Topological characteristics						Channel properties			
	$N$	$E$	$\langle k \rangle$	$\sigma_k^2/\langle k \rangle^2$	$C/C_{\text{rand}}$	$\langle l \rangle$	$\langle L \rangle$	$\sigma_L^2/\langle L \rangle^2$	$\langle S \rangle$	$\sigma_S^2/\langle S \rangle^2$
N1	49709	69563	2.80	0.165	763.7	73.05	6.47	0.362	12.03	2.51
N2	58618	82949	2.83	0.180	1000.4	74.67	5.94	0.348	11.53	6.66
N3	54083	76747	2.84	0.165	848.0	64.26	6.53	0.382	22.80	30.60
P1	33526	45544	2.72	0.162	488.2	69.61	6.85	0.401	19.18	3.23
P2	47388	66147	2.79	0.156	667.6	66.65	6.67	0.366	17.33	5.27
P3	27042	36125	2.67	0.165	368.3	70.73	7.15	0.450	21.31	4.00